Bioconjugate Chemistry

pubs.acs.org/bc

Article

Structural Optimization of Decoy Oligonucleotide-Based PROTAC That Degrades the Estrogen Receptor

Miyako Naganuma, Nobumichi Ohoka,* Genichiro Tsuji, Takao Inoue, Mikihiko Naito, and Yosuke Demizu*

Cite This: *Bioconjugate Chem.* 2023, 34, 1780−1788

Read Online

ACCESS | Metrics & More | Article Recommendations | Supporting Information

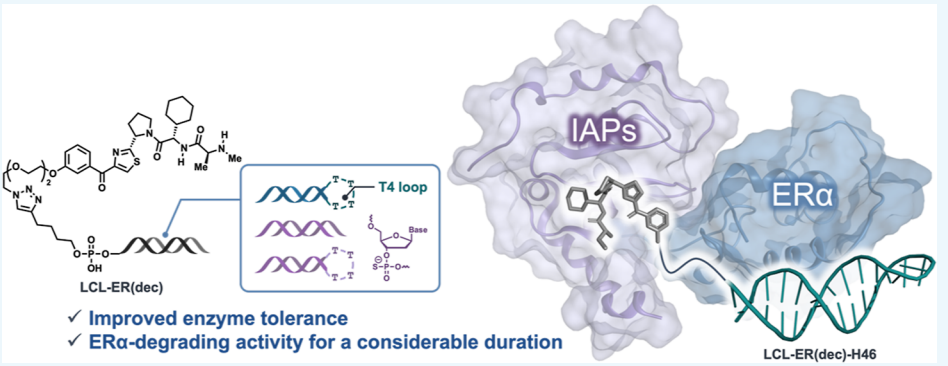

ABSTRACT: Proteolysis-targeting chimeras (PROTACs) have attracted attention as a chemical method of protein knockdown via the ubiquitin−proteasome system. Some oligonucleotide-based PROTACs have recently been developed for disease-related proteins that do not have optimal small-molecule ligands such as transcription factors. We have previously developed the PROTAC **LCL-ER(dec)**, which uses a decoy oligonucleotide as a target ligand for estrogen receptor α (ERα) as a model transcription factor. However, **LCL-ER(dec)** has a low intracellular stability because it comprises natural double-stranded DNA sequences. In the present study, we developed PROTACs containing chemically modified decoys to address this issue. Specifically, we introduced phosphorothioate modifications and hairpin structures into **LCL-ER(dec)**. Among the newly designed PROTACs, **LCL-ER(dec)-H46**, with a T4 loop structure at the end of the decoy, showed long-term ERα degradation activity while acquiring enzyme tolerance. These findings suggest that the introduction of hairpin structures is a useful modification of oligonucleotides in decoy oligonucleotide-based PROTACs.

INTRODUCTION

Chemical protein knockdown using proteolysis-targeting chimeras (PROTACs) is a powerful technology for degrading disease-related proteins by hijacking the endogenous ubiquitin−proteasome system (UPS).[1,2] PROTACs consist of three main components: a ligand for the target protein (warhead), a ligand for the ubiquitin E3 ligase, and a linker connecting the two ligands. PROTACs can degrade intracellular proteins such as protein kinases and transcription factors (TFs), including nuclear receptors and transcriptional regulators.[3,4] Although small-molecule warheads are the most commonly used approach in PROTAC development, the use of oligonucleotides as warheads has recently been developed.[5] This innovation expands the scope of PROTAC technology by allowing the recruitment of proteins of interest (POI) for which optimal small-molecule ligands have not yet been identified. Oligonucleotide-based PROTACs are advantageous in that ligands can be easily designed and synthesized (as long as the binding sequence to the POI is known). To date, several groups have described PROTACs that use RNA or DNA oligonucleotides.[6−9] Indeed, oligonucleotide-based PROTACs have great potential for targeting proteins that play critical roles in various diseases but lack optimal ligands such as TFs.

TFs are proteins that regulate gene expression by binding to specific DNA sequences, thereby controlling the chromatin structure and transcriptional activity.[10] The dysregulation of TFs has been implicated in various diseases, including many cancers.[11] With nearly 300 reported oncogenic TFs, accounting for approximately 20% of all known oncogenes, TFs are attractive targets for drug discovery. However, many of these proteins have complex structures, making it difficult to develop conventional small-molecule inhibitors.[11] Furthermore, be-

Received: July 23, 2023
Revised: September 12, 2023
Published: September 22, 2023

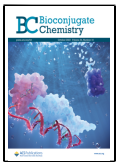

https://doi.org/10.1021/acs.bioconjchem.3c00332
Bioconjugate Chem. 2023, 34, 1780−1788

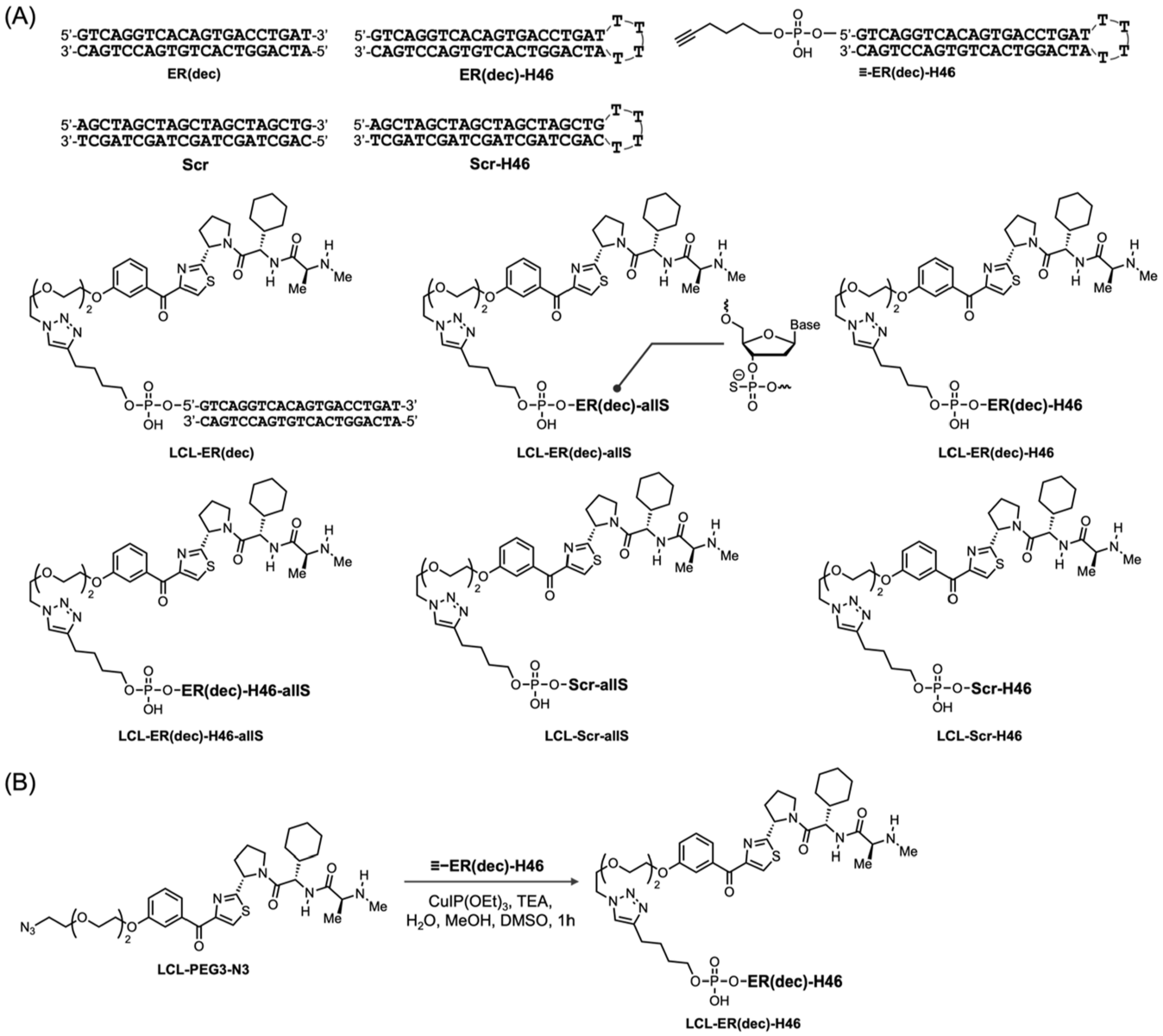

Figure 1. (A) PROTACs and decoy oligonucleotides developed in this study. (B) Synthetic scheme of a representative PROTAC, **LCL-ER(dec)-H46**.

cause the DNA-binding domain (DBD) sequences have been identified in approximately 96% of around 1600 human TFs,[10] PROTACs with molecular designs based on DNA-binding regions have been developed as a strategy to target TFs. TF-targeting chimeras (TRAFTACs), consisting of chimeric oligonucleotides that simultaneously bind the TF of interest and a HaloTag-fused dCas9 protein, were developed by Crews *et al.*[12] TRAFTACs recruit E3 ligases to the TF of interest via the intermediate protein dCas9HT7 in the presence of HaloPROTAC, and then, they degrade the TF of interest in a UPS-dependent manner. Furthermore, the chimeric molecule, TF-PROTAC, was developed by Wei *et al.* and consists of dozens of bases of decoy oligonucleotides targeting undruggable TFs that are linked to the E3 ligase ligand by a click reaction via a linker.[13] A similar concept, oligonucleotide PROTAC (O'PROTAC), was developed by Huang *et al.*; these O'PROTACs were able to degrade POI *in vivo* in mice with xenograft tumors.[14] At around the same time as these technologies were developed, we successfully developed **LCL-ER(dec)** as a decoy oligonucleotide-based PROTAC that targeted estrogen receptor α (ERα) as a model TF.[15] Three types of PROTACs—**LCL-ER(dec)** with LCL161 (E3 ligand for the inhibitor of apoptosis protein [IAP]), **VH-ER(dec)** with VH032 (E3 ligand for the von Hippel−Lindau protein), and **POM-ER(dec)** with pomalidomide (E3 ligand for cereblon)—were designed by conjugating the decoy oligonucleotide **ER(dec)** (which binds to ERα) and each E3 ligase ligand using the click reaction. Of these three PROTACs, **LCL-ER(dec)** had the greatest ERα degradation activity via the UPS.

Most decoy oligonucleotide-based PROTACs use natural DNA sequences. There is therefore a concern that they may be easily degradable by intracellular nucleases. A few PROTACs, such as RNA-PROTAC[6] and Oligo-TRAFTAC,[16] use phosphorothioate (PS)-modified oligonucleotides[17] (a common modification in oligonucleotide therapeutics) and

https://doi.org/10.1021/acs.bioconjchem.3c00332
Bioconjugate Chem. 2023, 34, 1780−1788

reportedly have therapeutic effects *in vivo*. One example of a PROTAC using oligonucleotides with a hairpin structure (a common structural modification of oligonucleotides) has also been reported.[13] Moreover, although there are several reports of decoy oligonucleotide-based PROTACs incorporating oligonucleotide modifications, comprehensive studies of their stability, target protein degradation activity, and target selectivity remain lacking. In the present study, we propose a PROTAC design with an incorporated T4 loop structure and a PS-modified oligonucleotide to enhance the chemical stability of our previously developed **LCL-ER(dec)**.

Decoy oligonucleotide strategies generally use relatively short double-stranded natural oligonucleotides that have low thermal stability under physiological conditions. An additional limitation is that decoy oligonucleotides are susceptible to degradation by extra- and intracellular nucleases. The presence of phosphate diester bonds within **LCL-ER(dec)** may also make it more susceptible to cleavage by these nucleases. To address these issues, we designed **LCL-ER(dec)-allS**, which incorporated a PS backbone into all bases. The introduction of additional nonbridging sulfur atoms in the internucleotide phosphate group provides enhanced stability against nucleases and is expected to improve cellular permeability.[18] Furthermore, there is a concern that **ER(dec)** of double-stranded decoy oligonucleotides may not show sufficient activity because intermolecular hydrogen bonds can form higher order structures and separate the two strands. The introduction of a T4 loop structure into a single-stranded DNA facilitates the formation of a stable hairpin structure and enhances the stability of higher order structures.[19] We therefore designed **LCL-ER(dec)-H46**, in which a four-residue T4 loop structure was introduced into **LCL-ER(dec)**. In addition, we designed **LCL-ER(dec)-H46-allS**, which contained both the PS modification and the T4 loop structure (Figure 1). We then assessed the resistance of these new PROTACs to DNA-degrading enzymes, as well as their binding activity to ERα. To further investigate the intracellular stability and activity of these PROTACs, we evaluated their ERα degradation activity and ERα-dependent transcriptional activity in MCF-7 breast cancer cells. Finally, we used the Molecular Operating Environment (MOE) software platform to calculate the ternary complex structures of ERα/cIAP1/PROTAC, thereby modeling their interactions.[20,21]

RESULTS AND DISCUSSION

The sense chain 5′-GTCAGGTCACAGTGACCTGAT-3′ of **ER(dec)**[15,22,23] was modified with a hexynyl group at the 5′-terminus, and LCL161 had a PEG3 linker with azidized ends. The aforementioned sense chain with an alkyne was then conjugated to LCL161 using a copper-catalyzed click reaction. Subsequent hybridization with the antisense strand 5′-ATCAGGTCACTGATGCCTGAC-3′ yielded the desired chimeric molecules **LCL-ER(dec)**. The synthesis process for **LCL-ER(dec)-allS**, **LCL-ER(dec)-H46**, and **LCL-ER(dec)-H46-allS** followed the same approach; the respective decoy oligonucleotide moieties were modified prior to conjugation (Figure 1).

The higher order structures of synthesized **LCL-ER(dec)**, **LCL-ER(dec)-allS**, **LCL-ER(dec)-H46**, and **LCL-ER(dec)-H46-allS** were analyzed using circular dichroism spectra. Each decoy exhibited a negative maximum around 240 nm and a positive maximum around 280 nm, indicating the formation of typical right-handed B-type duplex structures. Importantly, the chemical modification of **LCL-ER(dec)** did not have any impact on higher order structures (Figure S4).

The spectrophotometric determination of melting temperature (T_m) values in 25 mM salt revealed T_m values of 64.7, 53.0, 71.5, and 59.9 °C for **LCL-ER(dec)**, **LCL-ER(dec)-allS**, **LCL-ER(dec)-H46**, and **LCL-ER(dec)-H46-allS**, respectively. **LCL-ER(dec)-H46**, which was specifically designed to enhance the stability of higher order conformations, had a relatively high T_m value, indicating improved stability compared with **LCL-ER(dec)**. Conversely, the T_m values of the PS-modified PROTACs **LCL-ER(dec)-allS** and **LCL-ER(dec)-H46-allS** were lower than that of **LCL-ER(dec)**. The observed T_m values indicate a gradual reduction in duplex stability from **LCL-ER(dec)** to **LCL-ER(dec)-allS**, consistent with previous findings in monothioate strands (Table S2 and Figure S5).[18,24,25]

The binding affinities of **LCL-ER(dec)**, **LCL-ER(dec)-allS**, **LCL-ER(dec)-H46**, and **LCL-ER(dec)-H46-allS** against ERα were evaluated by using a competitive fluorescence polarization assay. For evaluation, the compound was added to a buffer system containing ERα and a **fluorescence polarization probe**, which had a fluorescein (FAM)-labeled **ER(dec)** at the 5′-end (Figure S1). The inhibitory concentration of the compound was determined by calculating the IC_{50} values, which were 128 nM for **LCL-ER(dec)**, 13.4 nM for **LCL-ER(dec)-sllS**, 16.5 nM for **LCL-ER(dec)-H46**, and 7.97 nM for **LCL-ER(dec)-H46-allS** (Table 1 and Figure S6). These results indicate that all of the modified decoys had improved binding activity to ERα compared to **LCL-ER(dec)**. These improvements may be attributed to the stabilized double strand along with the preservation of crucial structural elements for binding ERα.

Table 1. ERα Binding Affinity (IC_{50}) of LCL-ER(dec), LCL-ER(dec)-allS, LCL-ER(dec)-H46, and LCL-ER(dec)-H46-allS

entry	compound	IC_{50} (nM)
1	**LCL-ER(dec)**	128 ± 16.9
2	**LCL-ER(dec)-allS**	13.4 ± 1.52
3	**LCL-ER(dec)-H46**	16.5 ± 1.88
4	**LCL-ER(dec)-H46-allS**	7.97 ± 3.24

Oligonucleotides with cross-linked terminal structures typically maintain comparable binding activity toward a target protein. Indeed, the circular dichroism spectrum of **LCL-ER(dec)-H46** closely resembled that of **LCL-ER(dec)** despite the increased T_m value, indicating the successful preservation of the structural characteristics. The IC_{50} values for the binding activity of PS-modified **LCL-ER(dec)-allS** and **LCL-ER(dec)-H46-allS** to ERα were determined as 13.4 and 7.97 nM, respectively, which also suggests enhanced binding activity. These results indicate that the augmented hydrophobicity of PS-modified oligonucleotides (compared with natural oligonucleotides) may contribute to their enhanced binding activity to ERα. It has been suggested that PS-modified oligonucleotides might cause nonspecific protein binding, thus resulting in sequence-independent effects that limit many applications.[17,18]

We next assessed the nuclease resistance of natural, PS-modified, and hairpin-modified oligonucleotide-based PROTACs using exonuclease III, which targets both ends of the double strand and degrades from the ends. **LCL-ER(dec)** was completely degraded by exonuclease III, whereas **LCL-**

https://doi.org/10.1021/acs.bioconjchem.3c00332
Bioconjugate Chem. 2023, 34, 1780−1788

ER(dec)-H46 was less degraded than **LCL-ER(dec)**. Both **LCL-ER(dec)-allS** and **LCL-ER(dec)-H46-allS** were resistant to exonuclease III and remained undegraded (Figure 2).

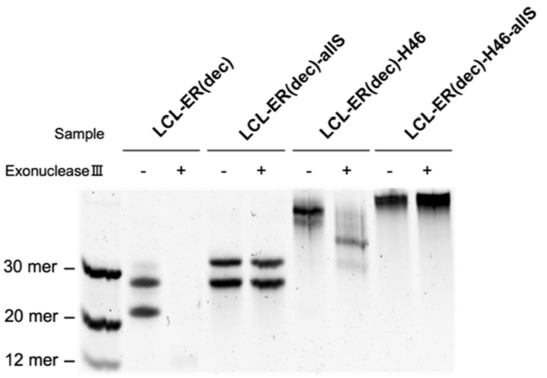

Figure 2. Nuclease-resistant properties of the synthesized PROTACs. **LCL-ER(dec)**, **LCL-ER(dec)-allS**, **LCL-ER(dec)-H46**, and **LCL-ER(dec)-H46-allS** were incubated with exonuclease III for 30 min. Full-length and digested oligonucleotides were resolved on 20% denaturing polyacrylamide gels.

Together, these results indicate that the incorporation of the hairpin structure and PS modification into a decoy PROTAC is a beneficial chemical modification that confers resistance to enzymatic degradation.

The cellular uptake efficiency of PROTACs was investigated by using various transfection reagents. To evaluate the intracellular transfection of the FAM-labeled decoy (**5′-FAM-ER(dec)**), flow cytometry analysis was performed using four different transfection reagents. First, MCF-7 cells were treated with 10 μM **5′-FAM-ER(dec)** and each transfection reagent for 24 h, and intracellular fluorescence intensities were then assessed. Compared with other transfection reagents, **5′-FAM-ER(dec)** was incorporated into cells most efficiently using Lipofectamine 2000 (Figure S7). Next, we prepared hairpin-type **5′-FAM-ER(dec)-H46** and PS-modified **5′-FAM-ER-(dec)-allS** and compared their cellular uptake with that of **5′-FAM-ER(dec)**. The hairpin-type **5′-FAM-ER(dec)-H46** exhibited a similar cellular uptake to **5′-FAM-ER(dec)**, whereas **5′-FAM-ER(dec)-allS** had a 19-fold higher cellular uptake (Figure 3). The enhanced cell membrane permeability of PS-modified decoy oligonucleotides may arise from their increased hydrophobicity and stronger binding affinity to membrane proteins.[18,26]

To assess the ERα degradation activity of **LCL-ER(dec)**, **LCL-ER(dec)-allS**, **LCL-ER(dec)-H46**, and **LCL-ER(dec)-H46-allS** against ERα, we conducted western blotting analysis in MCF-7 cells. After transfection, all PROTACs caused a decrease in ERα protein levels within 24 h; the hairpin-type **LCL-ER(dec)-H46** showed comparable ERα degradation activity to **LCL-ER(dec)** (Figure 4A). In contrast, PS-modified **LCL-ER(dec)-allS** and **LCL-ER(dec)-H46-allS** had adequate ERα degradation activity at concentrations approximately 100-fold lower (0.1 μM) than those of **LCL-ER(dec)** with natural oligonucleotides. This higher degradation activity may be attributed to improved cell membrane permeability and resistance to degradation by nucleases. In addition, these PS-modified PROTACs exhibited the hook effect, which is often observed with bifunctional molecules. Therefore, it should be noted that higher PROTAC concentrations likely inhibit efficient ternary complex formation, thus reducing the ability to degrade ERα.

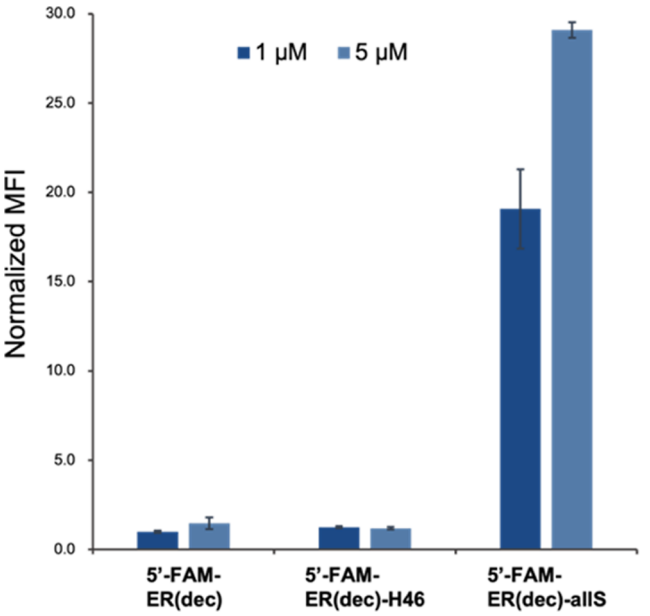

Figure 3. Evaluation of cellular uptake of hairpin-type **5′-FAM-ER(dec)-H46** and PS-modified **5′-FAM-ER(dec)-allS**. Values are the means and standard deviation of three independent cultures. Mean fluorescence intensities of the cells were normalized to those of **5′-FAM-ER(dec)**.

To investigate the impact of the DNA sequence on target ligand recognition by decoy molecules, we prepared LCL161 ligand−decoy chimeras using a scrambled DNA sequence (**Scr**) as the target ligand (Figure 1). Hairpin-type **LCL-Scr-H46** did not exhibit any ERα degradation activity. However, PS-modified **LCL-Scr-allS** showed marked ERα degradation activity (Figure 4B). The IC_{50} values for the binding of **LCL-Scr-allS** and **LCL-Scr-H46** to ERα were determined as 12.2 nM and >500 nM, respectively (Table S3). These results indicate that the ERα binding activity is consistent with the observed ERα degradation activity, suggesting that the PS modification may cause nonspecific binding to the protein. In contrast, **LCL-ER(dec)-H46** selectively degraded ERα in a sequence-specific manner. To investigate the selectivity of **LCL-ER(dec)-H46** for the target protein, we examined the effects of this PROTAC on the levels of different proteins. **LCL-ER(dec)-H46** did not reduce the levels of any other TFs (androgen receptor, aryl hydrocarbon receptor, or nuclear factor κB p65), transcription-related factors (bromodomain-containing protein 4), or nontranscription-related proteins (cellular retinoic acid binding protein 2, glyceraldehyde 3-phosphate dehydrogenase, or β-actin), indicating that this PROTAC selectively reduces ERα protein levels (Figure 4C).

Because PS-modified PROTACs showed relatively high enzyme tolerance but low target selectivity, we selected hairpin-type **LCL-ER(dec)-H46**, which showed relatively high enzyme tolerance and target selectivity, for the subsequent studies. To evaluate the sustainability of ERα degradation activity by PROTACs, a time course experiment was conducted. Although **LCL-ER(dec)** lost ERα degradation activity by 36 h after transfection, **LCL-ER(dec)-H46** showed ERα degradation activity up to 48 h (Figure 5). These results indicate that **LCL-ER(dec)-H46** exhibits sustained ERα degradation activity compared with **LCL-ER(dec)**.

https://doi.org/10.1021/acs.bioconjchem.3c00332
Bioconjugate Chem. 2023, 34, 1780−1788

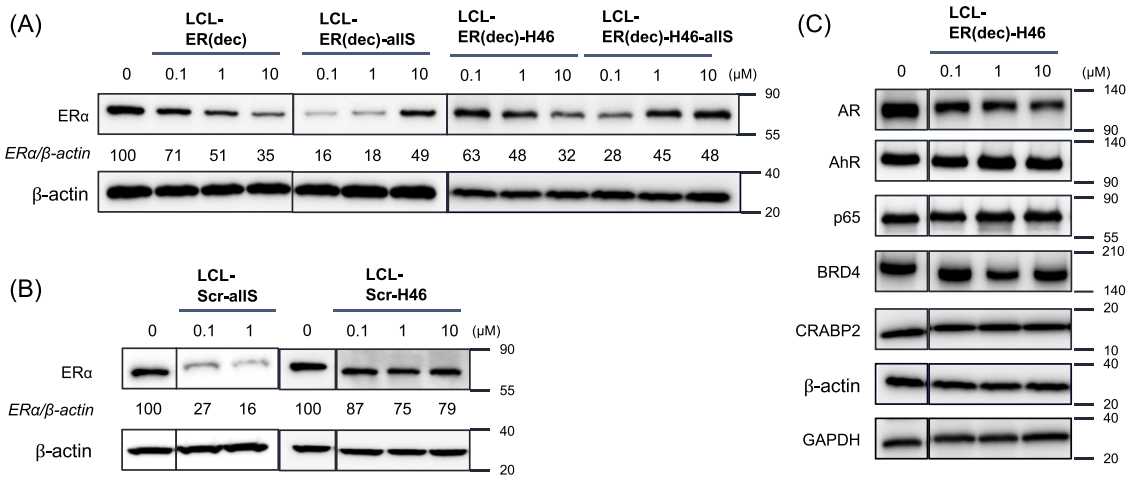

Figure 4. Degradation of ERα by synthesized PROTACs. (A) Synthesized PROTACs reduced ERα protein levels. (B) Degradation of ERα by **LCL-Scr-allS** and **LCL-Scr-H46**. MCF-7 cells were transiently transfected (for 24 h) with the indicated concentrations of **LCL-Scr-allS** and **LCL-Scr-H46**. (C) Degradation activity of **LCL-ER(dec)-H46** on several proteins. MCF-7 cells were transiently transfected (for 24 h) with the indicated concentrations of **LCL-ER(dec)-H46**. Whole-cell lysates were analyzed using western blotting with the indicated antibodies; representative data are shown. The numbers below the ERα panels represent the ERα/β-actin ratios, which were normalized by designating the expression under vehicle control (PROTAC-free) conditions as 100%. The changes in protein levels were reproducible over three independent experiments. Abbreviations: AhR, aryl hydrocarbon receptor; AR, androgen receptor; BRD4, bromodomain-containing protein 4; CRABP2, cellular retinoic acid binding protein 2; GAPDH, glyceraldehyde 3-phosphate dehydrogenase.

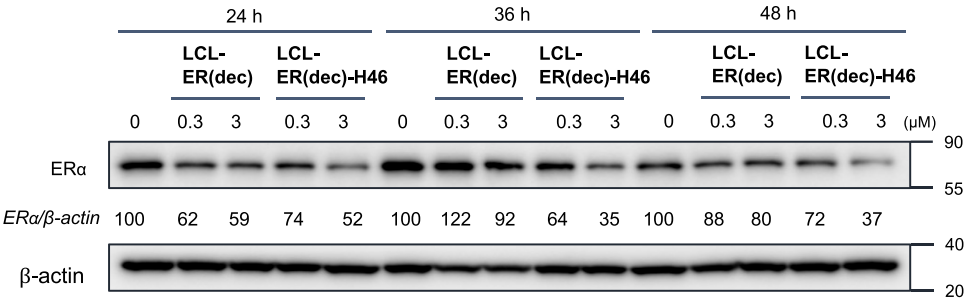

Figure 5. Time-dependent degradation of ERα by the synthesized PROTACs. MCF-7 cells were transfected with 0.3−3 μM **LCL-ER(dec)** and **LCL-ER(dec)-H46** and collected at the indicated time points for the western blotting analysis of ERα protein expression.

ERα plays an important role in estrogen signaling. The effects of **LCL-ER(dec)** and **LCL-ER(dec)-H46** on estrogen-dependent transcriptional activity were therefore evaluated using an estrogen-response-element-based reporter gene assay. When MCF-7 cells were treated with decoy PROTACs for 24 h, **LCL-ER(dec)-H46** inhibited β-estradiol (E2)-dependent transcriptional activation at levels comparable to **LCL-ER(dec)** in correlation with ERα degradation activity (Figure 6A). The antitumor effects of PROTACs on ERα-positive MCF-7 cells were also evaluated. In the cell viability assay, both **LCL-ER(dec)** and **LCL-ER(dec)-H46** had notable inhibitory effects on the MCF-7 cell viability. Furthermore, in correlation with ERα degradation activity, **LCL-ER(dec)-H46** effectively inhibited MCF-7 cell proliferation in a more time-dependent manner than **LCL-ER(dec)** (Figure 6B).

Finally, we used the MOE PROTAC modeling tool to generate models of the ERα/decoy-based PROTAC/cIAP1 ternary complex. The initial structures of the ternary complex were prepared using the cocrystal X-ray structures of the DBD of ERα and DNA (PDB: 1HCQ), and cIAP1 and the ligand (PDB: 3OZ1), following a previously reported method. The Amber14:EHT force field was used, and the DNA sequence bound to ERα was modified to a hairpin-type **ER(dec)-H46** sequence. Additionally, a PEG3 linker structure was introduced at the 5′-end of the sequence. In the case of cIAP1, the parent ligand was substituted with LCL161 for structural optimization of the complex. These initial structures were then subjected to modeling using Method 3B, which is an improved version of Method 3 of the PROTAC modeling tools and specifically designed for DNA-based PROTAC-mediated ternary complex modeling. The result showed that cIAP1 and ERα were in close proximity to each other via **LCL-ER(dec)-H46** and could form a stable ternary complex (Figure 7).

■ CONCLUSIONS

Decoy oligonucleotide-based PROTACs are a promising new technology for inducing the degradation of undruggable TFs. Natural oligonucleotide-based decoy PROTACs, which have been commonly used in the past, are unstable; their stability needs to be significantly improved for drug development. In the present study, we designed chemically modified decoy-based PROTACs—hairpin-type **LCL-ER(dec)-H46**, and PS-modified **LCL-ER(dec)-allS** and **LCL-ER(dec)-H46-allS**—to address this issue. These PROTACs exhibited enzyme resistance to exonuclease III, and PS-modified PROTACs exhibited particularly high enzyme resistance. Moreover, chemical modification of the oligonucleotides of **LCL-ER(dec)** significantly improved its binding activity to ERα. These

https://doi.org/10.1021/acs.bioconjchem.3c00332
Bioconjugate Chem. 2023, 34, 1780−1788

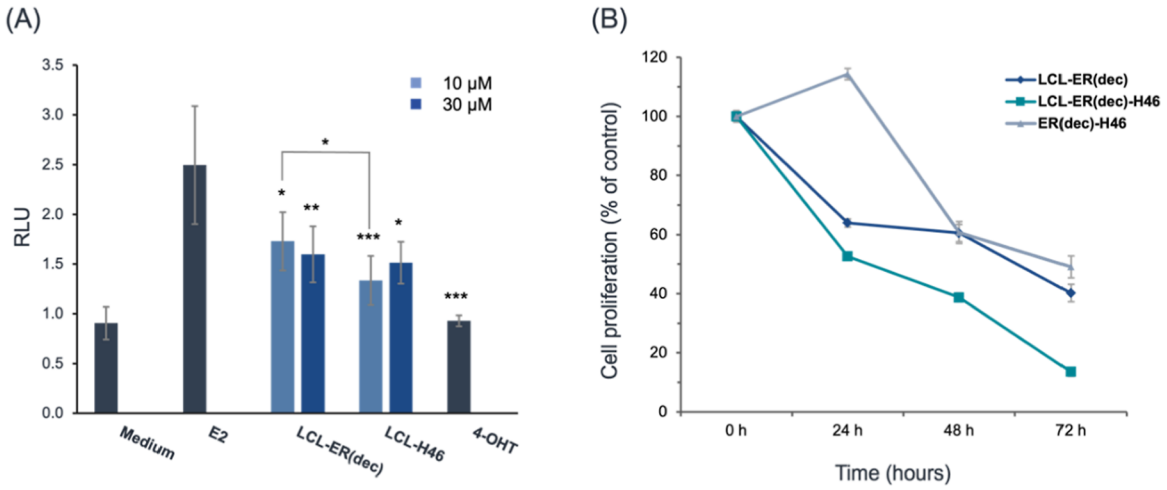

Figure 6. Effects of **LCL-ER(dec)-H46** on the estrogen-dependent transcriptional activity of ERα. (A) Inhibition of estrogen-dependent transcriptional activity of ERα by **LCL-ER(dec)-H46**. MCF-7 cells were transiently transfected with a luciferase reporter plasmid containing three tandem copies of the estrogen response element and control Renilla luciferase plasmid-SV40. After 24 h, the cells were further transfected for 24 h with 10−30 μM of the indicated decoys in the presence of 3 nM β-estradiol (E2). The ERα-dependent transcriptional activity was evaluated by luciferase assay, and relative luciferase activity was normalized by designating the activity of the nontreated control (column 1) as 100%. Data represent the mean ± standard deviation (n = 5). P-values were determined using the unpaired two-tailed Student's t-test. *P < 0.05; **P < 0.01; and ***P < 0.005. (B) Growth inhibition of ERα-positive breast cancer cells by **LCL-ER(dec)-H46**. MCF-7 cells were transfected with 10 μM of the indicated decoys for 24−72 h, and cell proliferation was then evaluated using a cell viability assay. Data represent the mean ± standard deviation (n = 5).

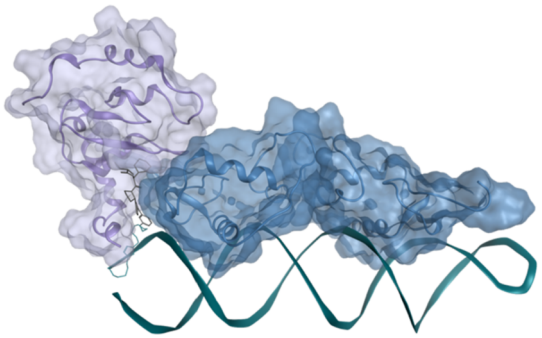

Figure 7. Ternary complex structure model of the DBD of ERα (blue), cIAP1(purple), and **LCL-ER(dec)-H46** (green). The ternary complex was modeled by using MOE 2022.02.

improvements may be caused by the hairpin modification-induced stabilization of higher order structure and the PS modification-induced increased hydrophobicity and enhanced interactions with ERα.

The hairpin-type **LCL-ER(dec)-H46** showed stable ERα degradation activity over 24 h of treatment. Moreover, PS-modified **LCL-ER(dec)-allS** had increased ERα degradation activity; however, these PROTACs had a reduced target selectivity. Together, these results suggest that PS modifications of oligonucleotides reduce target specificity. When we evaluated the time-dependent ERα degradation activities of **LCL-ER(dec)-H46** and **LCL-ER(dec)**, which selectively degrade ERα, **LCL-ER(dec)-H46** degraded ERα more continuously than **LCL-ER(dec)**. The sustained degradation of the ERα by **LCL-ER(dec)-H46** was further supported by the results of the effective estrogen signaling inhibitory activity. Chemical stabilization of the hairpin modification, by introducing the T4 loop, may contribute to these effects. This modification is therefore a useful approach for selectively degrading proteins using decoy oligonucleotides. *In silico* calculations demonstrated that cIAP1 and ERα are closely situated, potentially enabling the formation of a stable ternary complex through the **LCL-ER(dec)-H46** interaction.

Oligonucleotide modification in decoy-based PROTACs should be considered for their stability and target specificity and requires further investigation. Currently, the intracellular delivery of decoy oligonucleotide-based PROTACs involves the use of transfection reagents; therefore, the development of efficient intracellular delivery methods is therefore essential. Strategies to address the hurdles in this critical and unresolved issue include the use of drug delivery systems including cell membrane-permeable peptides and lipid nanoparticles. Overcoming these challenges will be crucial for unlocking the therapeutic potential of decoy-based PROTACs. Thus, although the concept of oligonucleotide-based PROTACs is promising, the field remains in its infancy; further research and development are required to refine and optimize approaches for their practical and safe clinical application.

EXPERIMENTAL SECTION

Oligonucleotide Synthesis. Decoys were synthesized on a 1.0 μmol scale using an automated DNA synthesizer (T-Series, Nihon Techno Service) by means of phosphoramidite chemistry with 5′-dimethoxytrityl-2′-deoxynucleoside phosphoramidites (Glen Research). To synthesize a sequence containing a hexynyl group at the 5′-end, synthesis continued according to the standard protocol, and 5′-hexynyl phosphoramidite (Glen Research) was used in the last coupling step to introduce a hexynyl group at the 5′-terminus. To synthesize fluorescein-labeled oligonucleotides, synthesis continued according to the standard protocol, and 6-fluorescein phosphoramidite (Sigma-Aldrich) was used in the last coupling step to introduce FAM dye at the 5′-terminus. The decoys on solid support (CPG) were treated with 28% ammonium hydroxide for 15 h at 55 °C and concentrated in vacuo. Deprotected decoys were purified by using reversed-phase HPLC. HPLC

https://doi.org/10.1021/acs.bioconjchem.3c00332
Bioconjugate Chem. 2023, 34, 1780−1788

conditions are as follows: Column: CAPCELL PAK MG-II (C18, 10 mm × 250 mm, 5 μm; OSAKA soda), mobile phase: A = 0.1 M triethylammonium acetate buffer (pH 7.0), B = CH_3CN. Gradient: B % = 10−40 over 20 min and 40−100 over 5 min. Flow rate: 10 mL/min, detection: 260 nm, column temperature: 35 °C. The concentration of the solution of decoys was determined using NanoDrop OneC (Thermo Fisher Scientific) by absorbance at 260 nm and molar absorbance coefficient (ε260) calculated from an OligoAnalyzer (IDT).

Synthesis of Chimeric Molecules by the Click Reaction. To a solution of IAP ligand (**LCL-PEG3-N3**[15]) in MeOH (10 mM, 300 μL, 3.0 μmol) was added the ERα-binding decoy **5′-hexynyl-ER(dec)-H46** in H_2O (2 mM, 700 μL, 1.4 μmol), TEA in DMSO (18 mM, 400 μL, 7.2 μmol), and $CuIP(OEt)_3$ in DMSO (38 mM, 400 μL, 15.2 μmol). The mixture was incubated at 40 °C for 1 h. The reaction mixture was purified by using HPLC and lyophilized. The collected oligo was precipitated in a solution of 0.3 M sodium acetate (pH 5.2)/70% ethanol to give the single strand of **LCL-ER(dec)**, which was resuspended in nuclease-free water to prepare a stock solution (1 mM, 840 μL, 0.84 μmol, 28%). Finally, the corresponding antisense strand was mixed in an aqueous solution and hybridized by heating at 95 °C for 10 min and gradually returning to room temperature to give the double-stranded title compound **LCL-ER(dec)**.

Denaturing DNA Polyacrylamide Gel Electrophoresis. Oligonucleotides were separated by 20% denaturing polyacrylamide gel [acrylamide/bis(acrylamide) = 19:1] electrophoresis (dPAGE) at 300 V for 30 min. dPAGE experiments were conducted using a 20% polyacrylamide gel (8 cm × 9 cm) containing 7 M urea and TBE buffer. Oligonucleotides (2 μM, 1 μL) were mixed with loading buffer (80% formamide, 20% TBE buffer, 4 μL) and heated at 95 °C for 5 min. Finally, the gels were imaged with UV illumination with a ChemiDoc Touch Imaging System (Bio-Rad).

Circular Dichroism Spectroscopy. Circular dichroism (CD) spectrum was recorded on a polarimeter (J-1100, JASCO) using a 0.1 cm path length cylindrical quartz cell. CD measurement conditions are as follows; concentration of decoys: 10 μM in TE buffer containing 25 mM NaCl pH 7.5, 25 °C.

T_m Measurement. Melting analysis of decoys was performed using a UV−vis spectrometer (V-730, JASCO) equipped with an 8-fold cuvette changer system with a 1.0 cm path length quartz. The duplex decoys (1 μM) were heated to 95 °C for 5 min and annealed in TE buffer (pH 7.5) containing 25 mM NaCl by slow cooling. The UV melting behavior was monitored at 260 nm from 35 to 85 °C at a rate of 1.0 °C/min. The melting temperature (T_m) of decoys was analyzed by the program provided with the measurement device. The data represent means and SD (n = 3).

Fluorescence Polarization Assay. Binding of test compounds to human ERα protein was measured using a fluorescence polarization assay (Invitrogen's protocol) containing recombinant ERα full-length protein (Invitrogen) and TE buffer (10 mM Tris−HCl and 1 mM EDTA, pH 7.5). ERα and fluorescein-labeled **FP-probe** were diluted with assay buffer to final concentrations of 100 and 0.05 nM, respectively, and 25 μL of the diluted solution was added to each well black low-volume assay plate (Greiner). Then, 25 μL of TE buffer containing the test substance was added to each well. After incubation at room temperature for 30 min, the fluorescence polarization signal (mP value) was measured using a plate reader equipped with a 480 nm excitation/635 nm emission filter (EnVision 2105, PerkinElmer). The data represent means and SD (n = 3).

Enzyme Tolerance Evaluation (dPAGE). Denaturing PAGE (dPAGE) experiments were conducted using a 20% polyacrylamide gel (8 cm × 9 cm) containing 7 M urea and TBE buffer. Electrophoresis was performed at a constant pressure of 200 V for 80 min. The gels were stained with a diluted solution of SYBR Green II dye in distilled water. For the cleavage of decoys by exonuclease III, a solution consisting of 1× NE buffer, 1 μM sample, and 4 units of exonuclease III (NEW ENGLAND BioLabs, M0206S) was incubated at 37 °C for 30 min. Subsequently, 12 mM EDTA was added to the solution, and the reaction was quenched by further incubation at 70 °C for 30 min. The above mixture (4 μL) was mixed with loading buffer (80% formamide, 20% TE buffer, 4 μL) and heated at 95 °C for 5 min. The resulting mixture was analyzed by dPAGE. Finally, the gels were imaged with UV illumination with a ChemiDoc Touch Imaging System (Bio-Rad).

Cell Culture and Transfection. Human breast carcinoma MCF-7 cells were purchased from ATCC (Manassas, VA) and maintained in RPMI 1640 medium (Sigma-Aldrich, St. Louis, MO, USA) containing 10% fetal bovine serum (FBS) and 100 U/mL penicillin and 100 μg/mL streptomycin (NACALAI TESQUE). To transfect the synthesized decoys, MCF-7 cells were seeded in 6-well plates at a density of 3.0×10^5 cells/well and cultured at 37 °C with an atmosphere of 5% CO_2. After 24 h, the cells were transfected with Lipofectamine 2000 Reagent (Thermo Fisher Scientific, Waltham, MA, USA) as follows. 125 μL of Opti-MEM I Reduced-Serum Medium (Gibco) with various concentrations of decoys were mixed with 125 μL of Opti-MEM with 4.5 μL of Lipofectamine 2000 (Invitrogen) and incubated at room temperature for 10 min. A total of 250 μL of the mixture was dropped into the culture wells and further incubated. After 24 h of incubation, the cells were harvested and subjected to western blot analysis.

Fluorescence-Activated Cell Sorting. To transfect the synthesized decoys, MCF-7 cells were seeded in 24-well plates at a density of 1.0×10^5 cells/well and cultured at 37 °C with an atmosphere of 5% CO_2 for 24 h. Then, the cells were washed three times with phosphate-buffered saline (PBS) supplemented with heparin (20 units/mL) and detached by treatment of trypsin−EDTA. The collected cells were pelleted by centrifugation at 3000 rpm for 5 min, and the supernatant was removed. The cells were washed twice with a PBS. Then, the collected cells were suspended in 500 μL of PBS, and mean fluorescence intensity in cells was measured by a flow cytometer (BD Accuri C6 Plus Flow Cytometer).

Western Blot Assay. Cells were washed with PBS, lysed with SDS lysis buffer (0.1 M Tris−HCl, pH 7.4, 10% glycerol, and 1% SDS), and immediately boiled for 10 min to obtain clear lysates. The protein concentration was measured by the BCA method (Thermo Fisher Scientific), and the lysates containing equal amounts of proteins were separated by SDS-PAGE and transferred to PVDF membranes (Merck Millipore Ltd.) for western blotting analysis using the appropriate antibodies. The immunoreactive proteins were visualized using the Clarity Western ECL substrate (Bio-Rad), and light emission intensity was quantified with a ChemiDocTMMP with Image Lab Software version 6.0.1 (Bio-Rad). The antibodies used in this study were anti-ERα antibody (Cell Signaling Technology, Danvers, MA, USA; 8644), anti-AR

https://doi.org/10.1021/acs.bioconjchem.3c00332
Bioconjugate Chem. 2023, 34, 1780−1788

antibody (Cell Signaling Technology, 5153), anti-AhR antibody (Cell Signaling Technology, 83200), anti-NF-κB p65 antibody (Cell Signaling Technology, 8242), anti-BRD4 antibody (Cell Signaling Technology, 13440), anti-GAPDH antibody (Santa Cruz, sc-47724 HRP), anti-CRABP2 antibody (Bethyl Laboratoreis, A300-809A), and anti-β-actin antibody (Sigma-Aldrich, A2228).

Dual Luciferase Reporter Gene Assay. MCF-7 cells were seeded in 96-well plates at a density of 1.0×10^4 cells/well and cultured for 24 h at 37 °C with an atmosphere of 5% CO_2. Then, the cells were transfected with firefly luciferase reporter plasmid containing three tandem copies of estrogen-response element and control Renilla luciferase plasmid-SV40 using Lipofectamine LTX (Invitrogen) in phenol red-free medium containing 4% charcoal/dextran-treated FBS. After 24 h, cells were treated with the indicated concentrations of **LCL-ER(dec)** or **LCL-ER(dec)-H46** with 4.5 μL of Lipofectamine 2000 in the presence of 3 nM β-estradiol in phenol red-free medium containing 0.2% charcoal/dextran-treated FBS for 24 h. The firefly luciferase activity in cell lysates was measured and normalized with Renilla luciferase activity. The data represent means and SD ($n = 5$).

Cell Proliferation Assay. MCF-7 cells were seeded in 96-well plates at a density of 5.0×10^3 cells/well and cultured for 24 h at 37 °C with an atmosphere of 5% CO_2. Then, the cells were transfected with various concentrations of decoys and Lipofectamine 2000 and cultured for 24−72 h. Cell viability was determined using water-soluble tetrazolium WST-8 (4-[3-(2-methoxy-4-nitrophenyl)-2-(4-nitrophenyl)-2*H*-5-tetrazolio]-1,3-benzene disulfonate) for the spectrophotometric assay according to the manufacturer's instructions (Dojindo). Cells treated with compounds were incubated with the WST-8 reagent for 1 h at 37 °C in a humidified atmosphere of 5% CO_2. The absorbance at 450 nm of the medium was measured using an Multiskan FC (Thermo Fisher Scientific).

Computational Analysis. All calculations and analyses were performed using MOE2022.02, and the force field was Amber14:EHT. The ERα DBD/decoy PROTAC/cIAP1 ternary complex model was constructed using Method 3B. Method 3B is a modified version of PROTAC Modeling Tools' Method 3 program that can also be used for decoy nucleotide PROTAC. This program was written in Scientific Vector Generator (SVL), which is integrated in the MOE modeling package and is freely available to MOE users from MOLSIS Inc. upon request. The structures required for ternary complex modeling are constructed as follows: For the cIAP1−LCL161 complex, LCL161 was docked into the complex of cIAP1 and its ligand (PDB: 3OZ1) prepared by MOE's QuickPrep, and the pose in which the linker attachment point faces outward from the binding site was selected. For the ERα−DNA complex, the DNA structure of the ERα−DNA complex (PDB: 1HCQ) prepared by MOE's QuickPrep was edited using MOE's DNA/RNA Builder. In addition, the linker structure of the PROTAC was added using MOE's Molecule Builder. These complexes were applied to Method 3B to construct several ternary complex models.

■ ASSOCIATED CONTENT

Supporting Information

The Supporting Information is available free of charge at https://pubs.acs.org/doi/10.1021/acs.bioconjchem.3c00332.

Synthetic procedures for all compounds and protocols for the *in vitro* assays (binding and protein degradation assays) (PDF)

■ AUTHOR INFORMATION

Corresponding Authors

Nobumichi Ohoka − *Division of Molecular Target and Gene Therapy Products, National Institute of Health Sciences, Kanagawa 210-9501, Japan;* orcid.org/0000-0002-0533-0610; Phone: +81-44-270-6537; Email: n-ohoka@nihs.go.jp; Fax: +81-44-270-6539

Yosuke Demizu − *Division of Organic Chemistry, National Institute of Health Sciences, Kanagawa 210-9501, Japan; Graduate School of Medical Life Science, Yokohama City University, Kanagawa 236-0027, Japan;* orcid.org/0000-0001-7521-4861; Phone: +81-44-270-6578; Email: demizu@nihs.go.jp; Fax: +81-44-270-6578

Authors

Miyako Naganuma − *Division of Organic Chemistry, National Institute of Health Sciences, Kanagawa 210-9501, Japan; Graduate School of Medical Life Science, Yokohama City University, Kanagawa 236-0027, Japan*

Genichiro Tsuji − *Division of Organic Chemistry, National Institute of Health Sciences, Kanagawa 210-9501, Japan;* orcid.org/0000-0002-2826-3852

Takao Inoue − *Division of Molecular Target and Gene Therapy Products, National Institute of Health Sciences, Kanagawa 210-9501, Japan*

Mikihiko Naito − *Laboratory of Targeted Protein Degradation, Graduate School of Pharmaceutical Sciences, The University of Tokyo, Tokyo 110-0033, Japan;* orcid.org/0000-0003-0451-1337

Complete contact information is available at: https://pubs.acs.org/10.1021/acs.bioconjchem.3c00332

Author Contributions

Miyako Naganuma, N.O., and G.T. performed the experiments and analyzed the results. Miyako Naganuma, N.O., T.I., M.N., and Y.D. designed the research and wrote the paper. All authors discussed the results and commented on the manuscript.

Notes

The authors declare no competing financial interest.

■ ACKNOWLEDGMENTS

We would like to express our deepest appreciation to Dr. Kentaro Kamiya (MOLSIS Inc.) for his help in the PROTAC modeling. This study was supported in part by grants from AMED under grant numbers 23mk0101197 (to Y.D.), 23ae0121013 (to Y.D.), 23ak0101185 (to Y.D.), 23mk0101220 (to Y.D.), 23fk0210110 (to Y.D.), 23fk0310506 (to Y.D.), 23ak0101186 (to T.I. and N.O.), and 23fk0310504 (to N.O.). The study also received support from the Japan Society for the Promotion of Science (KAKENHI, grants JP21K05320 to Y.D.; JP23H04926 to Y.D.; JP18H05502 to M.N. and Y.D.; JP18K06567 and JP21K06490 to N.O.; JP19K16333 to G.T.; and JP21H02777 and 22F22107 to M.N.; JSPS Fellows grant 21J23036 to Miyako Naganuma). We thank Bronwen Gardner, PhD, from Edanz (https://jp.edanz.com/ac) for editing a draft of this manuscript.

■ ABBREVIATIONS

PROTACs, proteolysis targeting chimeras; IAP, inhibitor of apoptosis protein; UPS, ubiquitin proteasome system; TF, transcription factor; ERa, estrogen receptor a; POI, protein of interest; DBD, DNA-binding domain; TRAFTACs, TRAnscription Factor TArgeting Chimeras; TOI, transcription factor of interest; VHL, von Hippel−Lindau protein; ERE, estrogen-responsive element; PS, phosphorothioate; MOE, molecular operating environment; FAM, fluorescein; CD, circular dichroism; T_m, melting temperature; RLU, relative light unit; DDS, drug delivery systems; CPP, cell membrane-permeable peptide; LNP, lipid nanoparticles; TEA, triethylamine

■ REFERENCES

(1) Bekes, M.; Langley, D. R.; Crews, C. M. PROTAC targeted protein degraders: the past is prologue. *Nat. Rev. Drug Discovery* **2022**, *21*, 181−200.

(2) Hu, Z.; Crews, C. M. Recent Developments in PROTAC-Mediated Protein Degradation: From Bench to Clinic. *Chembiochem* **2022**, *23*, No. e202100270.

(3) Zeng, S.; Huang, W.; Zheng, X.; Liyan, C.; Zhang, Z.; Wang, J.; Shen, Z. Proteolysis targeting chimera (PROTAC) in drug discovery paradigm: Recent progress and future challenges. *Eur. J. Med. Chem.* **2021**, *210*, 112981.

(4) He, M.; Cao, C.; Ni, Z.; Liu, Y.; Song, P.; Hao, S.; He, Y.; Sun, X.; Rao, Y. PROTACs: great opportunities for academia and industry (an update from 2020 to 2021). *Signal Transduction Targeted Ther.* **2022**, *7*, 181.

(5) Liu, Y.; Qian, X.; Ran, C.; Li, L.; Fu, T.; Su, D.; Xie, S.; Tan, W. Aptamer-Based Targeted Protein Degradation. *ACS Nano* **2023**, *17*, 6150−6164.

(6) Ghidini, A.; Clery, A.; Halloy, F.; Allain, F. H. T.; Hall, J. RNA-PROTACs: Degraders of RNA-Binding Proteins. *Angew. Chem., Int. Ed. Engl.* **2021**, *60*, 3163−3169.

(7) Patil, K. M.; Chin, D.; Seah, H. L.; Shi, Q.; Lim, K. W.; Phan, A. T. G4-PROTAC: targeted degradation of a G-quadruplex binding protein. *Chem. Commun.* **2021**, *57*, 12816−12819.

(8) Ji, J.; Ma, S.; Zhu, Y.; Zhao, J.; Tong, Y.; You, Q.; Jiang, Z. ARE-PROTACs Enable Co-degradation of an Nrf2-MafG Heterodimer. *J. Med. Chem.* **2023**, *66*, 6070−6081.

(9) Li, X.; Zhang, Z.; Gao, F.; Ma, Y.; Wei, D.; Lu, Z.; Chen, S.; Wang, M.; Wang, Y.; Xu, K.; et al. c-Myc-Targeting PROTAC Based on a TNA-DNA Bivalent Binder for Combination Therapy of Triple-Negative Breast Cancer. *J. Am. Chem. Soc.* **2023**, *145*, 9334−9342.

(10) Lambert, S. A.; Jolma, A.; Campitelli, L. F.; Das, P. K.; Yin, Y.; Albu, M.; Chen, X.; Taipale, J.; Hughes, T. R.; Weirauch, M. T. The Human Transcription Factors. *Cell* **2018**, *172*, 650−665.

(11) Lambert, M.; Jambon, S.; Depauw, S.; David-Cordonnier, M. H. Targeting Transcription Factors for Cancer Treatment. *Molecules* **2018**, *23*, 1479.

(12) Samarasinghe, K. T. G.; Jaime-Figueroa, S.; Burgess, M.; Nalawansha, D. A.; Dai, K.; Hu, Z.; Bebenek, A.; Holley, S. A.; Crews, C. M. Targeted degradation of transcription factors by TRAFTACs: TRAnscription Factor TArgeting Chimeras. *Cell Chem. Biol.* **2021**, *28*, 648−661.e5.

(13) Liu, J.; Chen, H.; Kaniskan, H. U.; Xie, L.; Chen, X.; Jin, J.; Wei, W. Y. TF-PROTACs Enable Targeted Degradation of Transcription Factors. *J. Am. Chem. Soc.* **2021**, *143*, 8902−8910.

(14) Shao, J.; Yan, Y.; Ding, D.; Wang, D.; He, Y.; Pan, Y.; Yan, W.; Kharbanda, A.; Li, H. Y.; Huang, H. Destruction of DNA-Binding Proteins by Programmable Oligonucleotide PROTAC (O'PROTAC): Effective Targeting of LEF1 and ERG. *Adv. Sci.* **2021**, *8*, No. e2102555.

(15) Naganuma, M.; Ohoka, N.; Tsuji, G.; Tsujimura, H.; Matsuno, K.; Inoue, T.; Naito, M.; Demizu, Y. Development of Chimeric Molecules That Degrade the Estrogen Receptor Using Decoy Oligonucleotide Ligands. *ACS Med. Chem. Lett.* **2022**, *13*, 134−139.

(16) Samarasinghe, K. T. G.; An, E.; Genuth, M. A.; Chu, L.; Holley, S. A.; Crews, C. M. OligoTRAFTACs: A generalizable method for transcription factor degradation. *RSC Chem. Biol.* **2022**, *3*, 1144−1153.

(17) Brown, D. A.; Kang, S. H.; Gryaznov, S. M.; DeDionisio, L.; Heidenreich, O.; Sullivan, S.; Xu, X.; Nerenberg, M. I. Effect of phosphorothioate modification of oligodeoxynucleotides on specific protein binding. *J. Biol. Chem.* **1994**, *269*, 26801−26805.

(18) Crinelli, R.; Bianchi, M.; Gentilini, L.; Magnani, M. Design and characterization of decoy oligonucleotides containing locked nucleic acids. *Nucleic Acids Res.* **2002**, *30*, 2435−2443.

(19) Nakane, M.; Ichikawa, S.; Matsuda, A. Triazole-linked dumbbell oligodeoxynucleotides with NF-kappa B binding ability as potential decoy molecules. *J. Org. Chem.* **2008**, *73*, 1842−1851.

(20) Drummond, M. L.; Williams, C. I. In Silico Modeling of PROTAC-Mediated Ternary Complexes: Validation and Application. *J. Chem. Inf. Model.* **2019**, *59*, 1634−1644.

(21) Drummond, M. L.; Henry, A.; Li, H.; Williams, C. I. Improved Accuracy for Modeling PROTAC-Mediated Ternary Complex Formation and Targeted Protein Degradation via New In Silico Methodologies. *J. Chem. Inf. Model.* **2020**, *60*, 5234−5254.

(22) Klein-Hitpaß, L.; Schorpp, M.; Wagner, U.; Ryffel, G. U. An estrogen-responsive element derived from the 5′ flanking region of the Xenopus vitellogenin A2 gene functions in transfected human cells. *Cell* **1986**, *46*, 1053−1061.

(23) Schwabe, J. W. R.; Chapman, L.; Finch, J. T.; Rhodes, D. The Crystal Structure of the Estrogen Receptor DNA-binding Domain Bound to DNA: How Receptors Discriminate between their Response Elements. *Cell* **1993**, *75*, 567−578.

(24) Jaroszewski, J. W.; Clausen, V.; Cohen, J. S.; Dahl, O. NMR Investigations of Duplex Stability of Phosphorothioate and Phosphorodithioate DNA Analogues Modified in Both Strands. *Nucleic Acids Res.* **1996**, *24*, 829−834.

(25) Wang, S. S.; Xiong, E.; Bhadra, S.; Ellington, A. D. Developing predictive hybridization models for phosphorothioate oligonucleotides using high-resolution melting. *PLoS One* **2022**, *17*, No. e0268575.

(26) Zhao, Q.; Matson, S.; Herrera, C. J.; Fisher, E.; Yu, H.; Krieg, A. M. Comparison of Cellular Binding and Uptake of Antisense Phosphodiester, Phosphorothioate, and Mixed Phosphorothioate and Methylphosphonate Oligonucleotides. *Antisense Res. Dev.* **1993**, *3*, 53−66.

https://doi.org/10.1021/acs.bioconjchem.3c00332
Bioconjugate Chem. 2023, 34, 1780−1788